JOURNAL OF CHEMICAL INFORMATION AND MODELING

Article

pubs.acs.org/jcim

Molecular Dynamics Investigation on a Series of HIV Protease Inhibitors: Assessing the Performance of MM-PBSA and MM-GBSA Approaches

Hemant Kumar Srivastava and G. Narahari Sastry*

Centre for Molecular Modelling, CSIR-Indian Institute of Chemical Technology, Tarnaka, Hyderabad 500 607, India

Supporting Information

ABSTRACT: The binding free energies (ΔG_{Bind}) obtained from molecular mechanics with Poisson−Boltzmann surface area (MM-PBSA) or molecular mechanics with Generalized Born surface area (MM-GBSA) calculations using molecular dynamics (MD) trajectories are the most popular procedures to measure the strength of interactions between a ligand and its receptor. Several attempts have been made to correlate the ΔG_{Bind} and experimental IC_{50} values in order to observe the relationship between binding strength of a ligand (with its receptor) and its inhibitory activity. The duration of MD simulations seems very important for getting acceptable correlation. Here, we are presenting a systematic study to estimate the reasonable MD simulation time for acceptable correlation between ΔG_{Bind} and experimental IC_{50} values. A comparison between MM-PBSA and MM-GBSA approaches is also presented at various time scales. MD simulations (10 ns) for 14 HIV protease inhibitors have been carried out by using the Amber program. MM-PBSA/GBSA based ΔG_{Bind} have been calculated and correlated with experimental IC_{50} values at different time scales (0−1 to 0−10 ns). This study clearly demonstrates that the MM-PBSA based ΔG_{Bind} (ΔG_{Bind}-PB) values provide very good correlation with experimental IC_{50} values (quantitative and qualitative) when MD simulation is carried out for a longer time; however, MM-GBSA based ΔG_{Bind} (ΔG_{Bind}-GB) values show acceptable correlation for shorter time of simulation also. The accuracy of ΔG_{Bind}-PB increases and ΔG_{Bind}-GB remains almost constant with the increasing time of simulation.

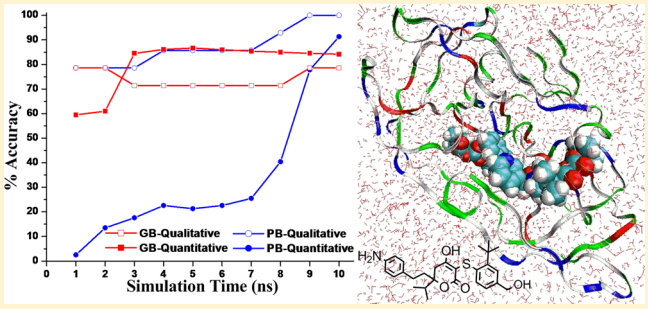

INTRODUCTION

The human immunodeficiency virus (HIV) is a retrovirus that infects cells of the human immune system and is responsible for the onset of the notorious disease called acquired immunodeficiency syndrome (AIDS). Currently around 34 million people live with AIDS and approximately 2.7 million people have been newly infected in the year 2010 alone.[1] Although the rate of new HIV infections has fallen and the number of AIDS-related deaths has decreased in recent years, the disease continues to be a major health concern especially in developing countries.[1] HIV protease was validated as a potential drug target in 1985, and the first X-ray crystal structure of the enzyme appeared in 1989.[2−4] HIV protease, a noncovalent homodimer, functions catalytically as an aspartic acid protease.[3,4] The chemical structure of all the FDA approved HIV protease inhibitors with brand name, generic name, date of FDA approval, and manufacturer name is depicted in Figure 1. Computational methods provided several major breakthroughs in the discovery of anti-HIV therapeutics.

Molecular docking methods efficiently dock the ligands in the active site of the receptor and provide good-quality binding poses but usually fail in accurately predicting the binding affinities.[5−7] The reason for such inconsistencies may be because the predicted binding affinity by molecular docking calculations is usually based on a single ligand−receptor complex structure and does not fully incorporate the protein flexibility.[7] Therefore docking fitness scores must be replaced with numbers obtained from thermodynamically appropriate binding contributions to get reliable results. Dynamic information in the energy calculations obtained by postprocessing methods is an alternative to docking based scoring functions. Postprocessing methods utilize the trajectory generated by MD or Monte Carlo (MC) simulations. Some of the most important post processing methods for free-energy estimation are free-energy perturbation (FEP),[8] thermodynamic integration (TI),[9] linear interaction energy analysis (LIE),[10] and MM-PBSA/GBSA calculations.[11,12] MM-PBSA/GBSA and LIE are very efficient computational approaches for the estimation of relative binding affinities.[13] Various computational methods to predict ΔG_{Bind} in ligand−receptor complexes have been reviewed.[14−19]

Jorgensen and co-workers studied the interactions and energetics associated with the binding of 20 HEPT and 20 nevirapine non-nucleoside HIV-1 reverse transcriptase inhibitors to understand simulation protocols and methods that can be used in the development of more effective anti-HIV drugs.[20] Jayaram and co-workers presented a computational method-

Received: August 17, 2012

   dx.doi.org/10.1021/ci300385h | J. Chem. Inf. Model. XXXX, XXX, XXX−XXX

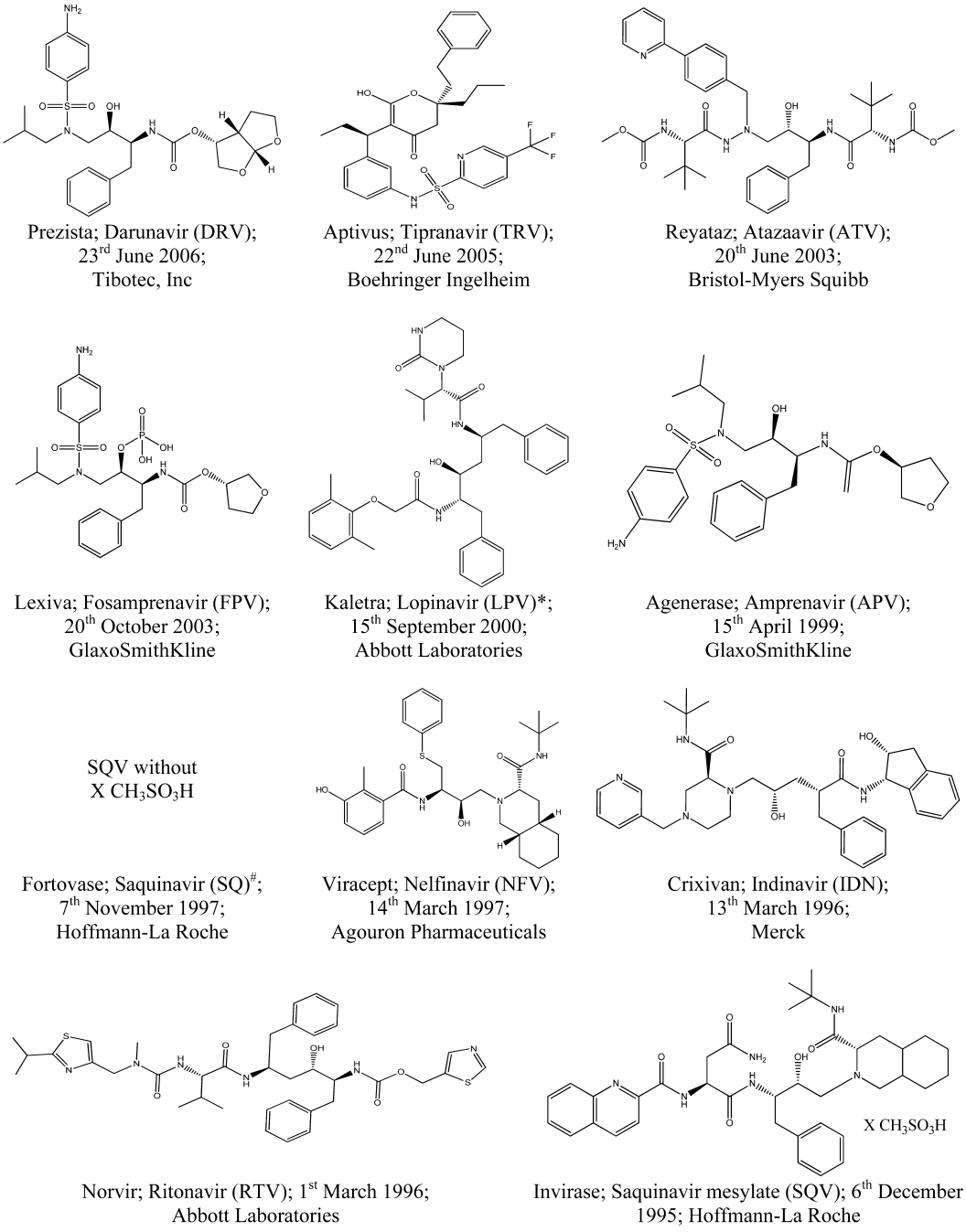

Figure 1. Chemical structure of all the FDA approved HIV protease inhibitors with brand name, generic name, date of FDA approval, and manufacturer name (*Saquinavir was withdrawn from the market in 2006. #Lopinavir is marketed only with Ritonavir).[73]

ology for the prediction of the ΔG_{Bind} of protein−ligand complexes by taking the complexes of HIV-1 protease with two peptidomimetic inhibitors as illustrative cases and performing 4 ns MD simulations.[21] Kuhn et al. validated the MM-PBSA approach on various ligands and eight different receptors to show that the application of MM-PBSA energy function to a single, relaxed complex structure is an adequate and sometimes more precise method compared to the standard free energy averaging over MD snapshots.[22] Hou et al. studied the binding of three inhibitors to both of the wild-type and the drug-resistant V82F/I84V mutant of the HIV-1 protease by MD simulations and MM-PBSA calculations.[23] Smith and co-workers estimated he ΔG_{Bind} for a series of 12 non-nucleoside TIBO inhibitors of HIV-1 reverse transcriptase by MC simulations and linear response approaches.[24] Docking, MD and linear interaction energy methods were used by Åqvist and co-workers to predict the binding modes and affinities for non-nucleoside inhibitors of HIV-1 reverse transcriptase.[25] Papadopoulos and co-workers performed all-atom MD simulations in explicit solvent and MM-PBSA calculations on four complexes (canagliflozin−HIV-1 protease, canagliflozin−renin, darunavir−renin, and aliskiren−HIV-1 protease) to show that the drugs currently used for the treatment of AIDS, hypertension, and diabetes could serve as dual inhibitors of HIV protease and renin.[26] The MM-PBSA technique was applied by Coveney and co-workers to rank the binding affinities of the saquinavir (protease inhibitor) to the wild-type and resistant variants of HIV-1 protease.[27] A different form of

dx.doi.org/10.1021/ci300385h | J. Chem. Inf. Model. XXXX, XXX, XXX−XXX

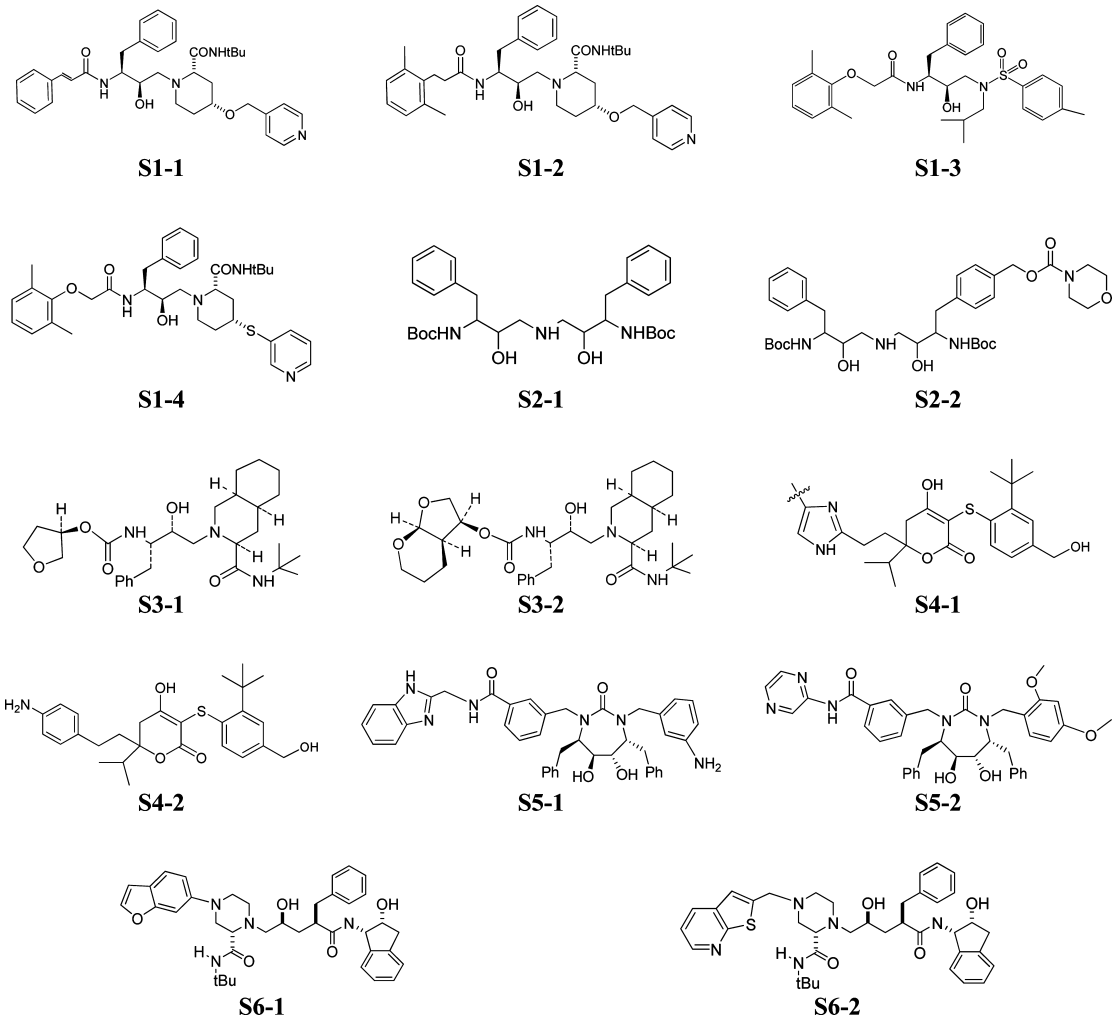

Figure 2. Chemical structure of all the protease inhibitors selected for the study. [2′,6′-dimethylphenoxyacetyl derivatives (S1), aminodiol derivatives (S2), tetrahydrofuran derivatives (S3), 4-hydroxy-5,6-dihydropyrone derivatives (S4), nonsymmetrically substituted cyclic ureacarboxamide derivatives (S5), and 3-pyridylmethyl-hydroxylaminpentenamide derivatives (S6)].

linear interaction energy approach was developed for the estimation of absolute ΔG_{Bind} on HIV protease inhibitors.[28−30]

Wang and co-workers applied structure-based computational approach to predict the mutants of HIV-1 protease resistant to the seven FDA approved drugs using molecular interaction energy components.[31] MD simulations and subsequent binding investigations were performed on six HIV-1 proteases complexed with FDA approved inhibitor lopinavir to understand whether relative ΔG_{Bind} of protein and ligand can be distinguished to a sufficient degree of accuracy by an enhancement of the MM-PBSA method.[32] Kollman and co-workers carried out a combined MD simulation and MM-PBSA calculation to rank the binding affinities of 12 TIBO-like HIV-1 reverse transcriptase inhibitors.[33] MD based ΔG_{Bind} values were also correlated with experimental values for DNA minor groove noncovalent[34,35] and covalent[36,37] binders. Knecht and co-workers performed MM-PBSA calculations to study the effectiveness of the HIV-1 protease inhibitors (darunavir, GRL-06579A, and GRL-98065) against HIV-2 and HIV-1 protease.[38] Wang and co-workers investigated the binding of darunavir (a protease inhibitor) to wild-type, single (I50V), and double (I50L/A71V) mutant HIV-proteases by MD simulations and MM-PBSA calculation.[39] Gasparrini and co-workers developed and validated a computational protocol to explore the orientational and conformational space of flexible selectors and selectands.[40,41] This protocol was further applied by Alcaro and co-workers to evaluate the interaction energies of HIV protease complexes.[42]

Accuracy of predicted ΔG_{Bind} values from ligand−receptor complex is necessary for efficiency in drug design and development. Once the methods are benchmarked, they become invaluable tools in screening new molecules reliably.[43,44] Several attempts have been made to calculate the values of ΔG_{Bind} and to correlate them with experimental numbers.[20−42] Clearly, most of the earlier studies are not exhaustive as they targeted either a small set of molecules or MD simulation times are not long enough. To our knowledge, a good agreement in between ΔG_{Bind} and IC_{50} values was not observed for a long series of the HIV protease inhibitors.

Therefore, in this manuscript, we resorted to undertake an exhaustive and systematic computational study which aims to obtain the correlation between the computed ΔG_{Bind}-PB/GB and experimental IC_{50} values. The appropriate time of MD simulation for such a correlation is also explored. We have collected six different scaffolds (S1-S6) of protease inhibitors from the literature with their experimental IC_{50} values and selected higher and lower active inhibitors (based on the IC_{50} values) for the study.[3,4,45−58] MD simulation for all 14 selected

dx.doi.org/10.1021/ci300385h | J. Chem. Inf. Model. XXXX, XXX, XXX−XXX

Table 1a. Comparison of Experimental IC_{50} Values with ΔG_{Bind}-PB at Various Time Scales of MD Simulation for Considered Inhibitors along with Number of Incorrect Trends (#E) and Correlation Coefficient (R^2 [a]) at Various Time Scales of MD Simulation

		ΔG_{Bind}-PB (kcal/mol)									
no.	IC_{50} (nM)	0−1 ns	0−2 ns	0−3 ns	0−4 ns	0−5 ns	0−6 ns	0−7 ns	0−8 ns	0−9 ns	0−10 ns
S1-1	4.959	−31.28	−34.57	−39.20	−40.67	−39.87	−38.53	−37.34	−35.60	−34.21	−33.95
S1-2	5.620	−40.49	−40.25	−40.54	−41.97	−42.50	−43.16	−44.53	−44.64	−44.76	−45.86
S1-3	8.585	−19.92	−18.64	−25.46	−29.52	−30.18	−32.29	−34.87	−40.58	−52.83	−59.76
S1-4	8.824	−56.02	−89.95	−93.35	−103.59	−92.84	−83.77	−77.69	−73.28	−71.70	−70.94
S2-1	6.398	−14.03	−15.89	−17.96	−20.64	−24.29	−26.82	−29.58	−30.57	−31.26	−31.86
S2-2	7.523	−81.18	−50.92	−64.36	−81.02	−93.49	−102.32	−108.34	−104.10	−96.16	−90.25
S3-1	6.159	−21.28	−21.47	−22.64	−22.46	−22.59	−23.68	−23.71	−23.33	−23.05	−23.65
S3-2	8.921	−26.18	−29.48	−30.75	−33.72	−33.61	−33.73	−32.67	−31.44	−30.69	−30.07
S4-1	7.155	−29.56	−28.60	−28.39	−27.84	−27.71	−28.27	−28.38	−28.38	−27.48	−26.79
S4-2	9.959	−24.63	−23.83	−26.69	−27.36	−27.59	−27.97	−28.28	−28.47	−29.34	−30.18
S5-1	7.973	−38.53	−37.69	−37.11	−35.12	−34.85	−34.56	−34.25	−34.45	−34.40	−34.29
S5-2	8.066	−37.79	−36.51	−35.09	−36.56	−37.93	−38.95	−39.58	−39.83	−40.19	−40.85
S6-1	8.770	−29.03	−27.26	−27.83	−28.08	−27.50	−27.74	−28.23	−28.04	−28.05	−28.19
S6-2	9.959	−32.35	−28.77	−27.96	−28.78	−30.51	−30.99	−31.16	−31.23	−31.77	−32.44
#E (qualitative)		3	3	3	2	2	2	2	1	0	0
R^2 (quantitative)		0.025	0.135	0.176	0.226	0.213	0.226	0.255	0.404	0.778	0.913

[a] R^2 is the correlation coefficient based on scaffold 1 because of different activity scales in various scaffolds.

inhibitors is carried out up to 10 ns times, and values of ΔG_{Bind}-PB/GB are calculated at the 10 different time intervals (0−1 to 0−10 ns). The ΔG_{Bind} values are correlated with experimental IC_{50} values at all the considered time scales for the purpose. A comparison between PBSA and GBSA approaches at different time scales is also carried out.

MATERIALS AND METHODS

Six different scaffolds of HIV protease inhibitors were selected from the reported literature viz. 2′,6′-dimethylphenoxyacetyl derivatives (S1),[45] aminodiol derivatives (S2),[46,47] tetrahydrofuran derivatives (S3),[48,49] 4-hydroxy-5,6-dihydropyrone derivatives (S4),[50−52] nonsymmetrically substituted cyclic ureacarboxamide derivatives (S5),[53] and 3-pyridylmethyl-hydroxylaminpentenamide derivatives (S6) along with their IC_{50} values.[54−58] Four inhibitors from S1 and ten inhibitors from others (S2-S6) were selected on the basis of variations in the IC_{50} values. Figure 2 depicts the chemical structure of all the selected scaffolds and inhibitors. Molecular docking studies were carried out on the GOLD (Genetic Optimization for Ligand Docking) program.[59] The MD simulation (with explicit solvent, involving ∼10 000 water molecules, see below) was performed up to 10 ns for the selected inhibitors using the Amber 8.0 program.[60−62] ΔG_{Bind}-PB and ΔG_{Bind}-GB values were estimated using MM-PBAS and MM-GBSA calculations, respectively.

MD Simulations. The Amber 8.0 program was used for MD simulations of the selected docked poses. The force field "leaprc.gaff" (generalized amber force field) was used to prepare the ligands, while "leaprc.ff03" was used for the receptor. The Amber force field was chosen because several examples in the literature use this force field for MD studies on various HIV protease inhibitors.[63−66] Each system was placed in a rectangular box (with a 10.0 Å boundry) of TIP3P water using the "SolvateOct" command with the minimum distance between any solute atom. Equilibration of the solvated complex was done by carrying out a short minimization (500 steps of each steepest descent and conjugate gradient method), 50 ps of heating, and 50 ps of density equilibration with weak restraints on the complex followed by 500 ps of constant pressure equilibration at 300 K. Adequate cutoff sizes are necessary to get reliable MD results, and therefore, a cutoff of 12.0 Å was used for MD simulations. All long-range electrostatics were included by means of a particle mesh Ewald (PME) method.[67] All hydrogen-heavy atom bonds were constrained by the SHAKE method, and simulations were performed with a 2 fs time step and langevin dynamics for temperature control. The same conditions as the final phase of equilibration were used for production run, and the coordinates were recorded in every 10 ps. The periodic boundary conditions (PBC) were used during MD simulations. Before submitting for the production run, we verified that the system is equilibrated. Root mean squared deviation (RMSD) plots were constructed for selected inhibitors using the Xmgrace program.

MM-PBSA and MM-GBSA Calculations. One-thousand equally spaced snapshots of each complex (every 10 ps) were generated from the MD trajectories, and all water molecules and counterions were removed before MM-PBSA/GBSA calculations. Coordinates were extracted by using the "extract_coords.mmpbsa" script and the ΔG_{Bind}-PB/GB values were calculated by using the "binding_energy.mmpbsa" script. These scripts were used ten times to calculate ΔG_{Bind} at ten different time scales (0−1 to 0−10 ns). The ΔG_{Bind}-PB/GB between a ligand and a receptor to form a complex can be calculated as follows.

$$\Delta G_{Bind} - PB/GB = \Delta E_{MM} + \Delta G_{SOL(PB/GB)} - T\Delta S$$

$$\Delta E_{MM} = \Delta E_{internal} + \Delta E_{electrostatic} + \Delta E_{vdw}$$

$$\Delta G_{SOL(PB/GB)} = \Delta G_{PB/GB} + \Delta G_{SA(PB/GB)}$$

where ΔE_{MM} is total gas phase energy (sum of $\Delta E_{internal}$ + $\Delta E_{electrostatic}$ + ΔE_{vdw}). $\Delta G_{SOL(PB/GB)}$ is sum of nonpolar and polar contributions to solvation calculated by PB or GB. $T\Delta S$ is conformational entropy upon binding computed by normal-mode analysis on a set of conformational snapshots taken from MD simulations. $\Delta E_{internal}$ is internal energy arising from bond, angle, and dihedral terms in the MM force field (this term

dx.doi.org/10.1021/ci300385h | J. Chem. Inf. Model. XXXX, XXX, XXX−XXX

Table 1b. Comparison of Experimental IC_{50} Values with ΔG_{Bind}-GB at Various Time Scales of MD Simulation for Considered Inhibitors along with Number of Incorrect Trends (#E) and Correlation Coefficient (R^2 [a]) at Various Time Scales of MD Simulation

		ΔG_{Bind}-GB (kcal/mol)									
no.	IC_{50} (nM)	0−1 ns	0−2 ns	0−3 ns	0−4 ns	0−5 ns	0−6 ns	0−7 ns	0−8 ns	0−9 ns	0−10 ns
S1-1	4.959	−64.34	−64.83	−68.65	−68.56	−68.11	−67.17	−66.53	−65.64	−65.08	−64.61
S1-2	5.620	−75.27	−76.26	−75.61	−75.96	−76.03	−75.83	−75.69	−75.03	−74.61	−74.03
S1-3	8.585	−55.74	−52.94	−51.77	−50.18	−48.31	−46.50	−45.43	−44.80	−44.73	−44.46
S1-4	8.824	−57.97	−57.98	−53.87	−51.15	−48.66	−47.06	−46.12	−45.31	−45.19	−45.18
S2-1	6.398	−48.80	−48.65	−49.49	−49.99	−50.65	−50.90	−51.17	−51.23	−51.61	−51.90
S2-2	7.523	−54.09	−49.17	−46.47	−45.01	−45.32	−45.39	−45.31	−44.66	−43.51	−42.66
S3-1	6.159	−55.99	−55.89	−55.87	−55.92	−56.06	−56.27	−56.52	−56.48	−56.46	−56.23
S3-2	8.921	−57.19	−59.38	−60.54	−61.41	−62.05	−61.83	−61.68	−60.78	−60.50	−59.98
S4-1	7.155	−58.02	−57.75	−58.21	−57.41	−57.30	−57.49	−57.29	−56.97	−55.84	−55.04
S4-2	9.959	−62.84	−63.77	−64.61	−64.77	−65.03	−65.10	−65.05	−64.84	−64.31	−63.51
S5-1	7.973	−65.81	−63.36	−62.16	−61.03	−60.77	−60.76	−60.38	−59.81	−59.37	−59.08
S5-2	8.066	−65.88	−64.89	−64.76	−64.52	−64.60	−64.79	−64.69	−64.62	−64.52	−64.51
S6-1	8.770	−69.93	−67.62	−66.51	−65.88	−65.57	−65.61	−65.28	−64.69	−64.43	−63.90
S6-2	9.959	−69.88	−65.75	−65.78	−65.10	−64.66	−64.53	−64.18	−64.30	−64.54	−64.76
#E (qualitative)		3	3	4	4	4	4	4	4	3	3
R^2 (quantitative)		0.595	0.610	0.845	0.861	0.867	0.860	0.854	0.850	0.845	0.843

[a] R^2 is the correlation coefficient based on scaffold 1 because of different activity scales in various scaffolds.

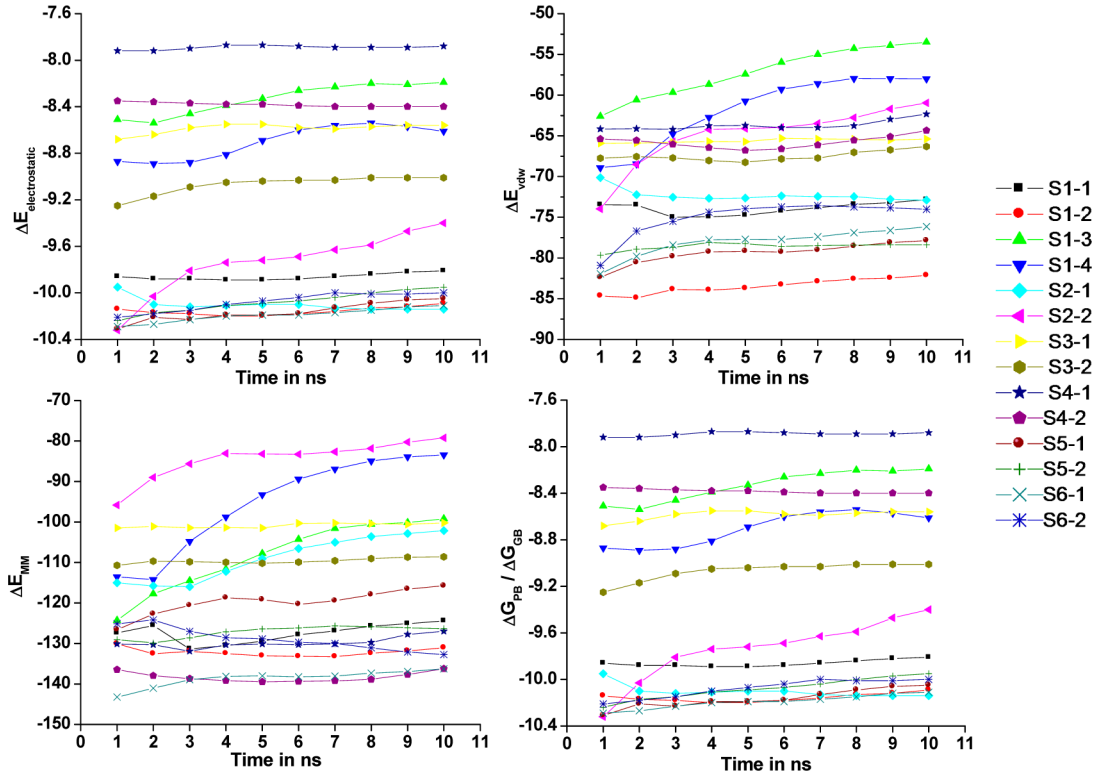

Figure 3. Plot depicting various components of ΔG_{Bind} at different time scales of MD simulation for all the considered inhibitors. [$\Delta E_{electrostatic}$ is electrostatic energy as calculated by the molecular mechanics (MM) force field. ΔE_{vdW} is van der Waals contribution from MM. $\Delta E_{internal}$ is internal energy arising from bond, angle, and dihedral terms in the MM force field (this term always amounts to zero in the single trajectory approach). ΔE_{MM} is total gas phase energy (sum of $\Delta E_{internal}$ + $\Delta E_{electrostatic}$ + ΔE_{vdw}). $\Delta G_{PB}/\Delta G_{GB}$ is nonpolar contribution to the solvation free energy calculated by an empirical model. See Supporting Information Tables S21−S23 for the values of various components of ΔG_{Bind}].

always amounts to zero in the single trajectory approach). $\Delta E_{electrostatic}$ is electrostatic energy as calculated by the molecular mechanics (MM) force field. ΔE_{vdw} is van der Waals contribution from MM. $\Delta G_{PB/GB}$ is nonpolar contribution to the solvation free energy calculated by an empirical model. $\Delta G_{SA\text{-}PB}$ and $\Delta G_{SA\text{-}GB}$ is the electrostatic contribution to the solvation free energy calculated by the PB or GB method, respectively.

Docking. The Sybyl 6.9.2 program (Tripos Inc., St. Louis, MO) was used for input preparation.[68] All the inhibitors were minimized to 0.001 kcal/(mol Å) root-mean-square gradients by using MMFF94 force field and point charges. Wild-type

dx.doi.org/10.1021/ci300385h | J. Chem. Inf. Model. XXXX, XXX, XXX−XXX

Table 2. Electrostatic Contribution to the Solvation Free Energy at Different Time Durations of MD Simulations Calculated by Both PB and GB Approaches

no.	0−1 ns	0−2 ns	0−3 ns	0−4 ns	0−5 ns	0−6 ns	0−7 ns	0−8 ns	0−9 ns	0−10 ns
	$\Delta G_{SA\text{-}PB}$ [the electrostatic contribution to the solvation free energy calculated by PB method]									
S1-1	106.00	100.83	102.02	99.74	99.43	99.21	99.41	99.95	100.75	100.27
S1-2	99.73	102.20	101.39	100.60	100.64	100.10	98.80	97.87	97.12	95.24
S1-3	112.86	107.64	97.48	90.47	85.94	80.25	74.92	68.19	55.53	47.64
S1-4	66.39	33.18	20.29	3.93	9.09	14.20	17.80	20.12	20.73	21.08
S2-1	110.93	109.98	108.13	101.71	94.88	89.84	85.58	83.16	81.71	80.42
S2-2	24.94	48.10	31.09	11.77	−0.58	−9.34	−16.04	−12.69	−6.41	−1.64
S3-1	88.88	88.24	87.38	87.47	87.47	85.19	85.14	85.64	86.06	85.15
S3-2	93.75	89.35	88.17	85.29	85.62	85.22	85.91	86.59	87.00	87.56
S4-1	108.50	109.63	111.41	110.41	110.30	109.92	109.61	109.27	108.18	108.06
S4-2	120.18	122.48	120.34	120.16	120.25	119.77	119.34	118.81	116.72	114.48
S5-1	98.38	95.23	93.71	93.81	94.52	95.92	95.37	93.57	92.23	91.53
S5-2	101.49	103.53	103.64	100.65	98.58	97.28	96.07	96.02	95.90	95.42
S6-1	124.50	124.04	121.35	120.26	120.66	120.69	119.98	119.44	119.01	118.18
S6-2	103.03	105.63	109.18	109.90	108.42	108.76	108.87	109.90	110.33	110.31
	$\Delta G_{SA\text{-}GB}$ [the electrostatic contribution to the solvation free energy calculated by GB method]									
S1-1	72.94	70.58	72.57	71.85	71.20	70.57	70.22	69.91	69.87	69.61
S1-2	64.96	66.44	66.49	66.73	67.20	67.52	67.71	67.54	67.32	67.12
S1-3	77.04	73.33	71.17	69.81	67.81	66.03	64.36	63.97	63.62	62.93
S1-4	64.44	65.15	59.77	56.37	53.27	50.91	49.36	48.09	47.24	46.84
S2-1	76.16	77.23	76.60	72.35	68.52	65.76	63.98	62.49	61.37	60.38
S2-2	52.02	49.84	48.99	47.78	47.59	47.59	46.99	46.75	46.23	45.95
S3-1	54.17	53.82	54.15	54.02	53.99	52.60	52.33	52.50	52.66	52.57
S3-2	62.73	59.44	58.38	57.60	57.18	57.11	56.89	57.25	57.20	57.65
S4-1	80.04	80.48	81.60	80.83	80.72	80.70	80.70	80.67	79.83	79.82
S4-2	81.98	82.55	82.43	82.76	82.81	82.64	82.58	82.45	81.75	81.15
S5-1	71.10	69.56	68.66	67.89	68.60	69.73	69.24	68.21	67.26	66.74
S5-2	73.41	75.16	73.97	72.69	71.90	71.44	70.96	71.23	71.58	71.77
S6-1	83.60	83.68	82.67	82.46	82.59	82.81	82.92	82.79	82.63	82.47
S6-2	65.49	68.64	71.35	73.58	74.27	75.22	75.85	76.82	77.56	77.98

HIV-1 protease (PDB ID 3NU3)[69] was used as a receptor for molecular docking calculations. The receptor was extracted from the complex, explicit hydrogens were added, and the energy minimization of hydrogens was carried out using 0.01 kcal/(mol Å) root-mean-squared gradient. Docking was performed using GOLD3.2 program that uses genetic algorithm (GA). This docking method allows a partial flexibility of receptor and full flexibility of ligand. For each of the 10 independent GA runs, a maximum number of 100 000 operations were performed with a population size of 100 individuals. Default values of niche size (2) and selection pressure (1.1) were used and operator weights for crossover, mutation, and migration were set to 95, 95, and 10, respectively. Default cutoff values of 2.5 Å for hydrogen bonds and 4.0 Å for van der Waals distance were employed. Best score docked poses were selected for MD simulations.

RESULTS AND DISCUSSION

This study is aimed to rigorously assess the performance MM-PBSA and MM-GBSA approaches, derived from MD simulations, for modeling HIV protease inhibitors. ΔG_{Bind} values of 14 HIV protease inhibitors (collected from six different scaffolds) are correlated with experimental IC_{50} values quantitatively and qualitatively, and reasonable simulation time is estimated for such correlations. In addition a systematic comparison of the performance of MM-PBSA and MM-GBSA approaches is also carried out. ΔG_{Bind}-PB/GB values are calculated at 10 different time scales (0−1 to 0−10 ns) and compared with the experimental IC_{50} values.

Table 1a shows the values of ΔG_{Bind}-PB at ten different time scales (0−1 to 1−10 ns) of MD simulation along with the IC_{50} values. With a view to ascertain the performance of ΔG_{Bind}-PB in qualitative terms, the number of incorrect trends have been periodically evaluated and depicted in Table 1a. It is pleasing to see that the number of incorrect trends decreases continuously as the length of simulation increases. It is three for 1−3 ns, two for 4−7 ns, one for 8 ns, and zero for 9 ns or higher time of simulation. The ΔG_{Bind}-PB values of each scaffold are correlated separately with the experimental IC_{50} values because IC_{50} values are at different scales for different scaffolds.[3,45−58] The quantitative correlation is measured on scaffold 1 (S1) which has four inhibitors in this study. There exists no correlation after 1 ns simulation time between the ΔG_{Bind}-PB and IC_{50} values (R^2 = 0.025). The correlation is rather poor up to 8 ns time (R^2 below 0.404), albeit a gradual increase was observed in the R^2 values with the increase in the time of simulation. Encouragingly, the correlation becomes excellent after 10 ns of simulation time.

Table 1b shows the ΔG_{Bind}-GB at 10 different time scales (0−1 to 1−10 ns) of MD simulation along with IC_{50} values. The number of occurrences of incorrect trends is three or four for all 10 time scales (0−1 to 0−10 ns) of the simulation in case of ΔG_{Bind}-GB, and in contrast to ΔG_{Bind}-PB, one did not encounter an increase in the correlation as the simulation time increases. The R^2 for ΔG_{Bind}-PB and ΔG_{Bind}-GB values is 0.025

dx.doi.org/10.1021/ci300385h | J. Chem. Inf. Model. XXXX, XXX, XXX−XXX

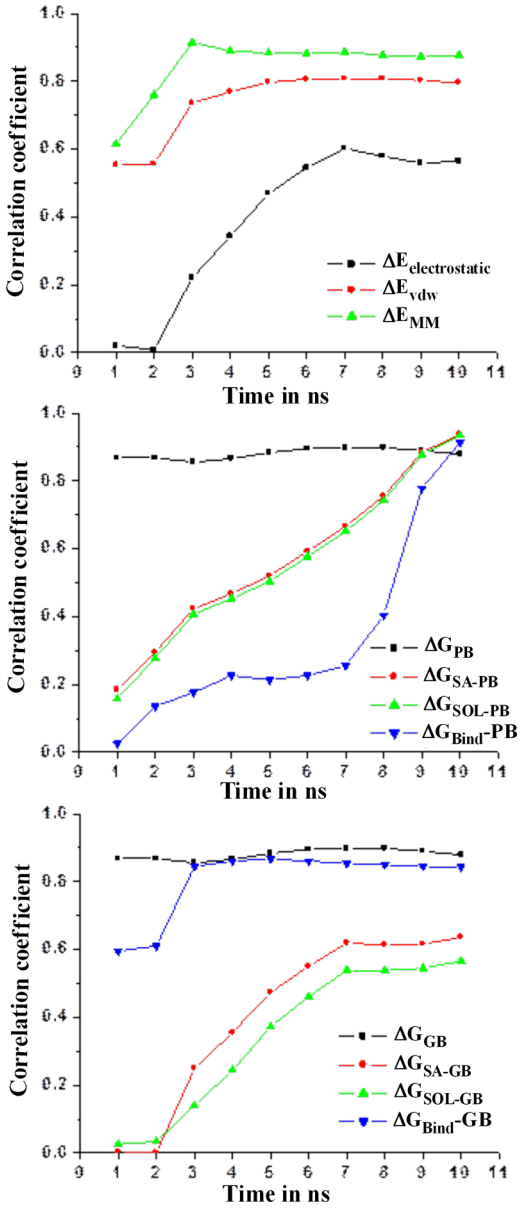

Figure 4. Plots of correlation coefficient values obtained by correlating ΔG_{Bind}-PB/GB and their components with experimental IC_{50} values at various time scales of MD simulations. [$\Delta E_{electrostatic}$ is electrostatic energy as calculated by the molecular mechanics (MM) force field. ΔE_{vdW} is van der Waals contribution from MM. $\Delta E_{internal}$ is internal energy arising from bond, angle, and dihedral terms in the MM force field (this term always amounts to zero in the single trajectory approach). ΔE_{MM} is total gas phase energy (sum of $\Delta E_{internal}$ + $\Delta E_{electrostatic}$ + ΔE_{vdW}). $\Delta G_{PB}/\Delta G_{GB}$ is nonpolar contribution to the solvation free energy calculated by an empirical model. $\Delta G_{SA\text{-}PB}/\Delta G_{SA\text{-}GB}$ is the electrostatic contribution to the solvation free energy calculated by PB or GB. $\Delta G_{SOL\text{-}PB}/\Delta G_{SOL\text{-}GB}$ is sum of nonpolar and polar contributions to solvation calculated by PB or GB. ΔG_{Bind}-PB/GB is final estimated binding free energies obtained by PB or GB method. See Supporting Information Table S24 for further details].

and 0.595, respectively, at 1 ns and 0.135 and 0.610, respectively, at 2 ns of simulation time which shows the higher accuracy for ΔG_{Bind}-GB values at lower simulation time. Acceptable quantitative correlation is observed at 2 ns or higher time of simulation (R^2 is ~0.85) for ΔG_{Bind}-GB values. Interestingly, the accuracy for ΔG_{Bind}-PB values at 10 ns is better compared to ΔG_{Bind}-GB values (0.913 and 0.843, respectively, for ΔG_{Bind}-PB and ΔG_{Bind}-GB based R^2 values).

The basic difference in the PB and GB approaches is the mode of the calculation of electrostatic contribution to the solvation free energy (ΔG_{SA}). The PB model is theoretically more rigorous compared to the GB model, and therefore, MM-PBSA is supposed to show higher accuracy compared to MM-GBSA for calculating the values of ΔG_{Bind}. ΔG_{SA} is calculated with a numerical solver for the PB method as implemented in the PBSA program[70] and for the GB method as implemented in sander.[60] In the GBSA approach, the solution to the electrostatic potential is replaced by an approximate calculation of the solvent-induced reaction field energy while in the PBSA approach the electrostatic potential remains accurate and thus PBSA is more time-consuming than GBSA. This may be one of the reasons why the percentage accuracy of results obtained from the PBSA approach continuously increases with the time of simulation while with GBSA approach it remains almost constant after 4 ns simulation. The values of ΔG_{Bind} are decomposed into contributions from van der Waals and electrostatic energies, nonpolar and electrostatic solvation free energies, and relative solute entropy effects in both PB and GB approaches. All the components of ΔG_{Bind} values were also correlated with IC_{50} values separately to see the impact and contribution of each component (see Supporting Information Tables S1-S20 for details) considering both the approaches.

Figure 3 shows the plots of various components of ΔG_{Bind} ($\Delta E_{electrostatic}$, ΔE_{vdw}, ΔE_{MM}, ΔG_{PB}) with respect to the time of MD simulations (see Table 2 for the values of $\Delta G_{SA\text{-}PB/GB}$ and Supporting Information Tables S21−S23 for the values of all the components). A quick look at Figure 3 indicates that the contribution of ΔE_{vdw} (average value −70.52) is higher compared to $\Delta E_{electrostatic}$ (average value −47.29) on the final estimated ΔG_{Bind}. Moreover $\Delta E_{electrostatic}$ and ΔE_{vdW} components always make a positive impact on the final estimated ΔG_{Bind}. The single trajectory approach is used to reduce the noise, and hence, there is no contribution from internal energy (arising from bond, angle and dihedral terms in the MM force field). Supporting Information Table S22 clearly shows that ΔG_{PB} component makes a positive impact while $\Delta G_{SA\text{-}PB}$ makes a negative impact (except in case of S2-2) on the final estimated ΔG_{Bind}. The contribution of $\Delta G_{SA\text{-}PB}$ (average value 87.99) is much higher compared to ΔG_{PB} (average value −9.38). In general, $\Delta G_{SA\text{-}PB}$ decreases continuously while ΔG_{PB} remains almost constant with respect to time during the simulation. Interestingly across different kinds of inhibitors, the ΔG_{PB} values show limited variation while $\Delta G_{SA\text{-}PB}$ values vary significantly. Supporting Information Table S23 shows that the contribution from ΔG_{GB} is positive while from $\Delta G_{SA\text{-}GB}$ is negative on the final estimated ΔG_{Bind}. The impact of $\Delta G_{SA\text{-}GB}$ (average value 67.74) is higher compared to ΔG_{PB} (average value −9.38). In addition, it is also clear from Table 2 that the effect of $\Delta G_{SA\text{-}GB}$ on the final estimated ΔG_{Bind} is minor compared to $\Delta G_{SA\text{-}PB}$. Thus, unlike electrostatic contribution, nonpolar contribution is not affected much with the time duration of simulation or with a change in the inhibitor in both PB and GB approaches. After analyzing the effect of various components, we have attempted to correlate each component separately with the IC_{50} values, Figure 4 (see Supporting Information Table S24 for details). Most of the components show a reasonable correlation which systematically improves, except $\Delta G_{PB/GB}$, with higher simulation time.

dx.doi.org/10.1021/ci300385h | J. Chem. Inf. Model. XXXX, XXX, XXX−XXX

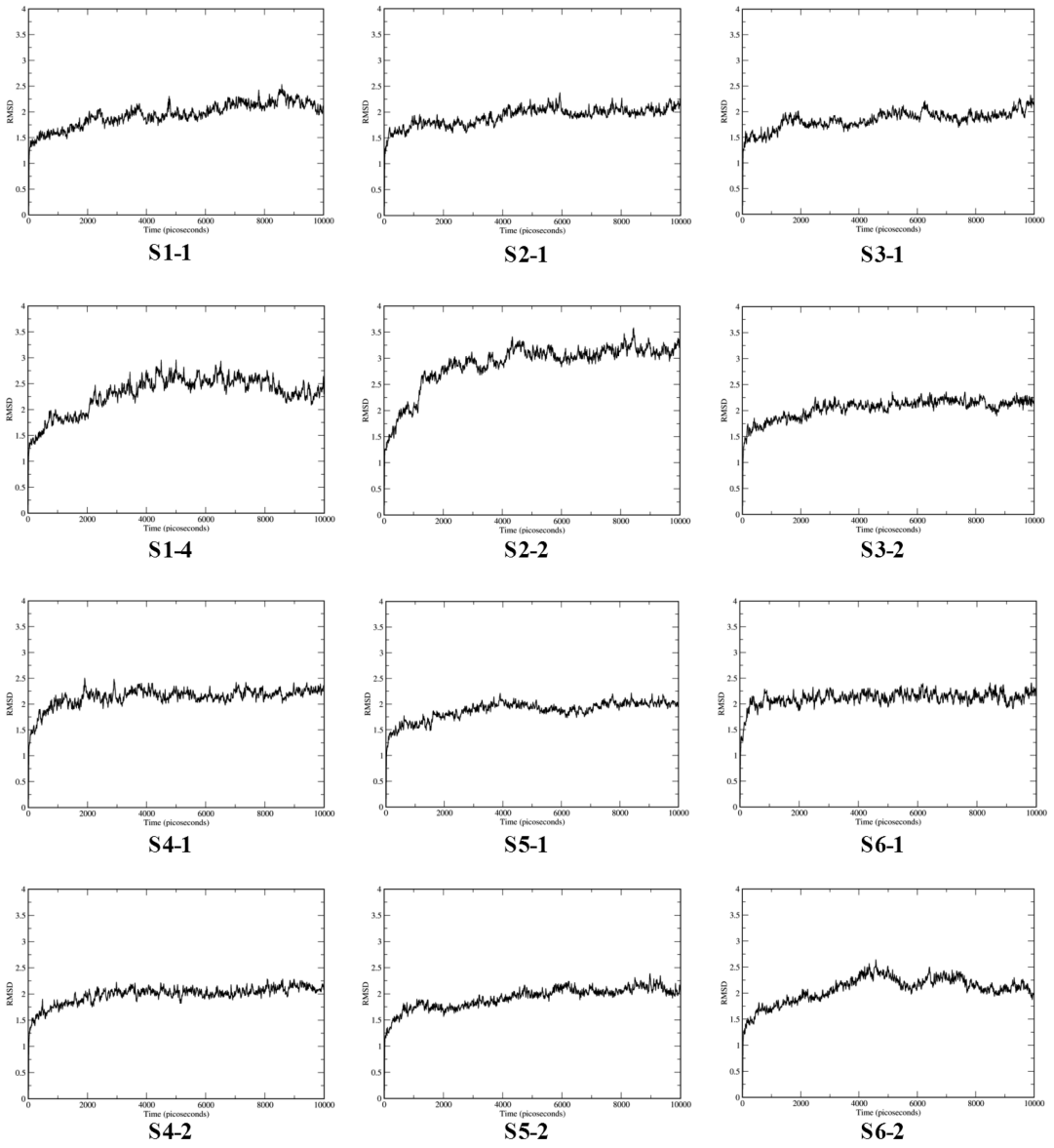

Figure 5. Plot of RMSD (in ångstrom) with respect to time in picoseconds for lowest and highest active inhibitors of each scaffold during 10 ns MD simulation.

The R^2 values for $\Delta G_{SA\text{-}PB}$ increases consistently from 1 to 10 ns simulation and $\Delta G_{SA\text{-}GB}$ increases only up to 6 ns. Perhaps, this explains why there is a lack of systematic improvement in the GBSA as the simulation time goes beyond 6 ns, which is in contrast with the PBSA method. The average deviation in $\Delta G_{SA\text{-}PB}$ is more (97.11, 95.72, 92.54, 88.30, 86.80, 84.34, 83.99, 83.20, and 82.41, respectively, for 1−10 ns) compared to $\Delta G_{SA\text{-}GB}$ (70.01, 69.71, 69.20, 68.34, 67.69, 67.19, 66.72, 66.48, 66.15, and 65.93, respectively, for 1−10 ns) during the simulation. The electrostatic contribution to the solvation free energy values increases continuously up to 10 ns in PBSA approach while in GBSA approach it increases up to 5−6 ns and then becomes constant. Supporting Information Tables S11−S20 contain the changes in ΔG_{Bind}-PB/GB and its components during the simulation and show that the changes are not based on the inhibitory activity. Figure 5 shows the RMSD plots with respect to time for the lowest and highest active inhibitors of each scaffold. These plots show that ligands remain bound to the receptor near the preferential binding position and experience fewer fluctuations during the simulations with respect to its initial placement. However a correlation between inhibitory activity and RMSD is not observed. Figure 6 illustrates the snapshots at different time scale for a selected inhibitor (S1-1) representative of the behavior of this class of compounds during the simulation. This figure also provides the RMSD values for complex and ligand at different time scales during the simulation with respect to the structure at 0 ns. The RMSD values were estimated by superimposition of complex and ligand separately.[71] With reference to the initial structure, a maximum RMSD of 2 and 1 Å are observed, respectively, for complex and free ligand during the simulation. A cursory examination of Figure 6 reveals that both receptor and ligand are fairly rigid and do not show high structural deviations during the simulation. Although higher ΔG_{Bind} may lead to a better inhibitory activity, it is important to mention that several other issues are also essential in the process of successful drug discovery, e.g. drug specificity, oral bioavailability, toxicity, drug-related side effects, drug resistance,

dx.doi.org/10.1021/ci300385h | J. Chem. Inf. Model. XXXX, XXX, XXX−XXX

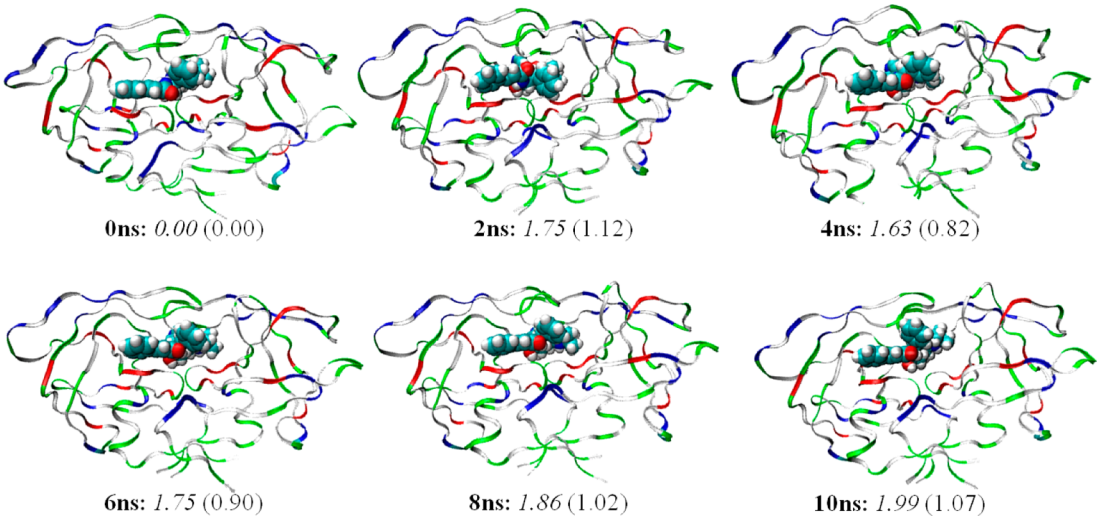

Figure 6. Snapshots at various time scales during the simulation and RMSD values of complex (in italics) and ligand (in parentheses) with respect to the structure at 0 ns for S1-1 inhibitor at different time scales of simulation.

etc.[72] One should note that the performance of PBSA and GBSA approaches is system dependent and extra care and further validation seems to be necessary to generalize the current findings for other class of scaffolds and inhibitors.

CONCLUSIONS

MM-PBSA and MM-GBSA approaches have been validated for modeling HIV protease inhibitors. Fourteen selected inhibitors from six different scaffolds were considered for the study, and 10 ns MD simulations were carried out. Following this, MM-PBSA/GBSA calculations were made at 10 different time scales (0−1 to 0−10 ns). It has been observed that the experimental IC_{50} values are comparable to the values of ΔG_{Bind}-PB/GB. Thus, the stronger binding may lead to the higher inhibitory activity for the selected classes of protease inhibitors. These results are in contrast to previous docking based results which conclude that the stability of protease inhibitors is not comparable with their inhibitory activity. A systematic comparison between MM-PBSA and MM-GBSA approaches has been carried out to test the applicability of these approaches for protease inhibitors. Qualitatively the number of incorrect trends decreases with the time of simulation (1−10 ns) in the PBSA approach while it remains almost constant in the GBSA approach. Quantitative correlation for this class of inhibitors is meaningful only after 9 ns in PBSA and after 3 ns in GBSA approaches. Thus, the PBSA approach shows much more accurate correlation (qualitatively and quantitatively) when longer time simulation is performed; however, the GBSA approach provides acceptable correlation even for lower nanosecond level simulation. The difference between GBSA and PBSA approaches is the increasing accuracy of the values of electrostatic contribution to the solvation free energy up to 10 ns for the PB approach and almost constant accuracy for the GB approach during the simulation. Quantitative statistical analysis is carried out for all the components of the binding free energy which indicates that the electrostatic contribution to the solvation free energy calculated by the PB method correlates very well with the experimental IC_{50} values. While one may obtain better correlation with GBSA compared to PBSA at shorter simulation time, the correlation with the PBSA approach will certainly be more reliable when simulations are run for sufficiently longer time.

ASSOCIATED CONTENT

Supporting Information

Comparison of experimental IC_{50} values with ΔG_{Bind}-PB/GB and their components at sequential intervals of MD simulation (Tables S1−S20) along with correlation coefficient (R^2). Absolute values of components of ΔG_{Bind} and correlation coefficient values obtained by correlating ΔG_{Bind}-PB/GB and their components with experimental IC_{50} values at different time scales of simulation for considered inhibitors. This material is available free of charge via Internet at http://pubs.acs.org.

AUTHOR INFORMATION

Corresponding Author

*E-mail: gnsastry@gmail.com. Phone: +91 40 27193016. Fax: +91 40 27160512.

Notes

The authors declare no competing financial interest.

ACKNOWLEDGMENTS

H.K.S. thanks the Department of Science and Technology (DST), New Delhi, for financial assistance through the Fast-Track (SR/FT/CS-031/2009) project. We thank DBT and CSIR, New Delhi, for funding and support.

REFERENCES

(1) World AIDS Day report 2011: UNIAIDS. www.unaids.org (accessed August 16, 2012).

(2) Srivastava, H. K.; Bohari, M. H.; Sastry, G. N. Modeling anti-HIV compounds: The role of analogue based approaches. *Curr. Comput. Aided Drug Des.* **2012**, *8*, 224−248.

(3) Srivastava, H. K.; Choudhury, C.; Sastry, G. N. The efficacy of conceptual DFT descriptors and docking scores on the QSAR models of HIV protease inhibitors. *Med. Chem.* **2012**, *8*, 811−825.

(4) Wlodawer, A.; Gustchina, A. Structural and biochemical studies of retroviral proteases. *Biochim. Biophys. Acta* **2000**, *1477*, 16−34.

(5) Warren, G. L.; Andrews, C. W.; Capelli, A. M.; Clarke, B.; LaLonde, J.; Lambert, M. H.; Lindvall, M.; Nevins, N.; Semus, S. F.; Senger, S.; Tedesco, G.; Wall, I. D.; Woolven, J. M.; Peishoff, C. E.;

Head, M. S. A Critical Assessment of Docking Programs and Scoring Functions. *J. Med. Chem.* **2006**, *49*, 5912−5931.
(6) Ferrara, P.; Gohlke, H.; Price, D. J.; Klebe, G.; Brooks, C. L., III Assessing Scoring Functions for Protein−Ligand Interactions. *J. Med. Chem.* **2004**, *47*, 3032−3047.
(7) Srivani, P.; Srinivas, E.; Raghu, R.; Sastry, G. N. Molecular modeling studies of pyridopurinone derivatives—Potential phosphodiesterase 5 inhibitors. *J. Mol. Graph. Model.* **2007**, *26*, 378−390.
(8) Zwanzig, R. W. High-Temperature Equation of State by a Perturbation Method. I. Nonpolar Gases. *J. Chem. Phys.* **1954**, *22*, 1420−1426.
(9) Kirkwood, J. G. Statistical mechanics of fluid mixtures. *J. Chem. Phys.* **1935**, *3*, 300−313.
(10) Aqvist, J.; Medina, C.; Samuelsson, J. E. A new method for predicting binding affinity in computer-aided drug design. *Protein Eng.* **1994**, *7*, 385−391.
(11) Srinivasan, J.; Miller, J.; Kollman, P. A.; Case, D. A. Continuum Solvent Studies of the Stabilities of RNA Hairpin Loops and Helices. *J. Biomol. Struct. Dyn.* **1998**, *16*, 671−682.
(12) Kollman, P. A.; Massova, I.; Reyes, C.; Kuhn, B.; Huo, S.; Chong, L.; Lee, M.; Lee, T.; Duan, Y.; Wang, W.; Donini, O.; Cieplak, P.; Srinivasan, J.; Case, D. A.; Cheatham, T. E., III Calculating Structures and Free Energies of Complex Molecules: Combining Molecular Mechanics and Continuum Models. *Acc. Chem. Res.* **2000**, *33*, 889−897.
(13) Lill, M. A.; Thompsan, J. J. Solvent Interaction Energy Calculations on Molecular Dynamics Trajectories: Increasing the Efficiency Using Systematic Frame Selection. *J. Chem. Inf. Model.* **2011**, *51*, 2680−2689.
(14) Ajay; Murcko, M. A. Computational Methods to Predict Binding Free Energy in Ligand-Receptor Complexes. *J. Med. Chem.* **1995**, *38*, 4953−4967.
(15) Jorgensen, W. L. Free energy changes in solution. In *Encyclopedia of Computational Chemistry*; Schleyer, P. v. R., Ed.; Wiley: New York, 1998; Vol. *2*, pp 1061−1070.
(16) Kollman, P. A. Free Energy Calculations: Applications to Chemical and Biochemical Phenomena. *Chem. Rev.* **1993**, *93*, 2395−2417.
(17) Gilson, M. K.; Given, J. A.; Bush, B. L.; McCammon, J. A. The statistical-thermodynamic basis for computation of binding affinities: a critical review. *Biophys. J.* **1997**, *72*, 1047−1069.
(18) Jorgensen, W. L. Free Energy Calculations: A Breakthrough for Modeling Organic Chemistry in Solution. *Acc. Chem. Res.* **1989**, *22*, 184−189.
(19) Simonson, T.; Georgios, A.; Karplus, M. Free Energy Simulations Come of Age: Protein-Ligand Recognition. *Acc. Chem. Res.* **2002**, *35*, 430−437.
(20) Rizzo, R. C.; Tirado-Rives, J.; Jorgensen, W. L. Estimation of Binding Affinities for HEPT and Nevirapine Analogues with HIV-1 Reverse Transcriptase via Monte Carlo Simulations. *J. Med. Chem.* **2001**, *44*, 145−154.
(21) Kalra, P.; Reddy, T. V.; Jayaram, B. Free Energy Component Analysis for Drug Design: A Case Study of HIV-1 Protease−Inhibitor Binding. *J. Med. Chem.* **2001**, *44*, 4325−4338.
(22) Kuhn, B.; Gerber, P.; Schulz-Gasch, T.; Stahl, M. Validation and Use of the MM-PBSA Approach for Drug Discovery. *J. Med. Chem.* **2005**, *48*, 4040−4048.
(23) Hou, T.; Yu, R. Molecular Dynamics and Free Energy Studies on the Wild-Type and Double Mutant HIV-1 Protease Complexed with Amprenavir and Two Amprenavir-Related Inhibitors: Mechanism for Binding and Drug Resistance. *J. Med. Chem.* **2007**, *50*, 1177−1188.
(24) Smith-Jr., R. H.; Jorgensen, W. L.; Tirado-Rives, J.; Lamb, M. L.; Janssen, P. A. J.; Michejda, C. J.; Smith, M. B. K. Prediction of Binding Affinities for TIBO Inhibitors of HIV-1 Reverse Transcriptase Using Monte Carlo Simulations in a Linear Response Method. *J. Med. Chem.* **1998**, *41*, 5272−5286.
(25) Carlsson, J.; Boukharta, L.; Åqvist, J. Combining Docking, Molecular Dynamics and the Linear Interaction Energy Method to Predict Binding Modes and Affinities for Non-nucleoside Inhibitors to HIV-1 Reverse Transcriptase. *J. Med. Chem.* **2008**, *51*, 2648−2656.
(26) Tzoupis, H.; Leonis, G.; Megariotis, G.; Supuran, C. T.; Mavromoustakos, T.; Papadopoulos, M. G. Dual Inhibitors for Aspartic Proteases HIV-1 PR and Renin: Advancements in AIDS−Hypertension−Diabetes Linkage via Molecular Dynamics, Inhibition Assays, and Binding Free Energy Calculations. *J. Med. Chem.* **2012**, *55*, 5784−5796.
(27) Stoica, I.; Sadiq, S. K.; Coveney, P. V. Rapid and Accurate Prediction of Binding Free Energies for Saquinavir-Bound HIV-1 Proteases. *J. Am. Chem. Soc.* **2008**, *130*, 2639−2648.
(28) Zoete, V.; Michielin, O.; Karplus, M. Protein-ligand binding free energy estimation using molecular mechanics and continuum electrostatics. Application to HIV-1 protease inhibitors. *J. Comput. Aided Mol. Des.* **2003**, *17*, 861−880.
(29) Alves, C. N.; Martí, S.; Castillo, R.; Andrés, J.; Moliner, V.; Tuñón, I.; Silla, E. A Quantum Mechanics/Molecular Mechanics Study of the Protein−Ligand Interaction for Inhibitors of HIV-1 Integrase. *Chem.—Eur. J.* **2007**, *13*, 7715−7724.
(30) Saen-oon, S.; Kuno, M.; Hannongbua, S. Binding Energy Analysis for Wild-Type and Y181C Mutant HIV-1 RT/8-Cl TIBO Complex Structures: Quantum Chemical Calculations Based on the ONIOM Method. *Proteins* **2005**, *61*, 859−869.
(31) Hou, T.; Zhang, W.; Wang, J.; Wang, W. Predicting drug resistance of the HIV-1 protease using molecular interaction energy components. *Proteins* **2009**, *74*, 837−846.
(32) Sadiq, S. K.; Wright, D. W.; Kenway, O. A.; Coveney, P. V. Accurate Ensemble Molecular Dynamics Binding Free Energy Ranking of Multidrug-Resistant HIV-1 Proteases. *J. Chem. Inf. Model.* **2010**, *50*, 890−905.
(33) Wang, J.; Morin, P.; Wang, W.; Kollman, P. A. Use of MM-PBSA in Reproducing the Binding Free Energies to HIV-1 RT of TIBO Derivatives and Predicting the Binding Mode to HIV-1 RT of Efavirenz by Docking and MM-PBSA. *J. Am. Chem. Soc.* **2001**, *123*, 5221−5230.
(34) Srivastava, H. K.; Chourasia, M.; Kumar, D.; Sastry, G. N. Comparison of Computational Methods to Model DNA Minor Groove Binders. *J. Chem. Inf. Model* **2011**, *51*, 558−571.
(35) Srivastava, H. K.; Sastry, G. N. Efficient Estimation of MMGBSA Based Binding Energies for DNA and Aromatic Furan Amidino Derivatives. *J. Biomol. Struct. Dyn.* **2012**, DOI: 10.1080/07391102.2012.703071.
(36) Kamal, A.; Bharathi, E. V.; Ramaiah, M. J.; Dastagiri, D.; Reddy, J. S.; Viswanath, A.; Sultana, F.; Pushpavalli, S.N.C.V.L.; Pal−Bhadra, M.; Srivastava, H. K.; Sastry, G. N.; Juvekar, A.; Sen, S.; Zingde, S. Quinazolinone linked Pyrrolo[2,1-c][1,4]benzodiazepine (PBD) Conjugates: Design, Synthesis and Biological Evaluation as Potential Anticancer Agents. *Bioorg. Med. Chem.* **2010**, *18*, 526−542.
(37) Kamal, A.; Shankaraiah, N.; Reddy, C. R.; Prabhakar, S.; Markandeya, N.; Srivastava, H. K.; Sastry, G. N. Synthesis of bis-1,2,3-triazolo-bridged unsymmetrical pyrrolobenzodiazepine trimers via 'click' chemistry and their DNA-binding studies. *Tetrahedron* **2010**, *66*, 5489−5506.
(38) Kar, P.; Knecht, V. Origin of Decrease in Potency of Darunavir and Two Related Antiviral Inhibitors against HIV-2 Compared to HIV-1 Protease. *J. Phys. Chem. B* **2012**, *116*, 2605−2614.
(39) Meher, B. R.; Wang, Y. Interaction of I50V Mutant and I50L/A71V Double Mutant HIV-Protease with Inhibitor TMC114 (Darunavir): Molecular Dynamics Simulation and Binding Free Energy Studies. *J. Phys. Chem. B* **2012**, *116*, 1884−1900.
(40) Alcaro, S.; Gasparrini, F.; Incani, O.; Caglioti, L.; Pierini, M.; Villani, C. "Quasi Flexible" Automatic Docking Processing for Studying Stereoselective Recognition Mechanisms, Part 2: Prediction of DDG of Complexation and 1H-NMR NOE Correlation. *J. Comput. Chem.* **2000**, *21*, 515−530.
(41) Alcaro, S.; Gasparrini, F.; Incani, O.; Mecucci, S.; Misiti, D.; Pierini, M.; Villani, C. A "Quasi-Flexible" Automatic Docking Processing for Studying Stereoselective Recognition Mechanisms. Part I. Protocol Validation. *J. Comput. Chem.* **2007**, *28*, 1119−1128.

(42) Alcaro, S.; Artese, A.; Ceccherini-Silberstein, F.; Ortuso, F.; Perno, C. F.; Sing, T.; Svicher, V. Molecular Dynamics and Free Energy Studies on the Wild-Type and Mutated HIV-1 Protease Complexed with Four Approved Drugs: Mechanism of Binding and Drug Resistance. *J. Chem. Inf. Model.* **2009**, *49*, 1751−1761.
(43) Badrinarayan, P.; Sastry, G. N. Virtual High-throughput Screening in new Lead Identification. *Comb. Chem. High Through. Scr.* **2011**, *14*, 840−860.
(44) Reddy, A. S.; Pati, S. P.; Kumar, P. P.; Pradeep, H. N.; Sastry, G. N. Virtual screening in drug discovery: A computational perspective. *Curr. Protein Pept. Sci.* **2007**, *8*, 329−351.
(45) Beaulieu, P. L.; Anderson, P. C.; Cameron, D. R.; Croteau, G.; Gorys, V.; Maitre, C. G.; Lamarre, D.; Liard, F.; Paris, W.; Plamondon, L.; Soucy, F.; Thibeault, D.; Wernic, D.; Yoakim, C.; Pav, S.; Tong, L. 2′,6′-Dimethylphenoxyacetyl: A New Achiral High Affinity P_3-P_2 Ligand for Peptidomimetic-Based HIV Protease Inhibitors. *J. Med. Chem.* **2000**, *43*, 1094−1108.
(46) Barrish, J. C.; Gordon, E.; Alam, M.; Lin, P. F.; Bisacchi, G. S.; Chen, P.; Cheng, P. T. W.; Fritz, A. W.; Greytok, J.;A.; Hermsmeier, M. A.; Humphreys, W. G.; Lis, K. A.; Marella, M. A.; Merchant, Z.; Mitt, T.; Morrison, R. A.; Obermier, M. T.; Pluscec, J.; Skoog, M.; Slusarchyk, W. A.; Sperge, S. H.; Stevenson, J. M.; Sun, C.; Sundeen, J. E.; Taunk, P.; Tino, J. A.; Warrack, B. M.; Colonno, R. J.; Zahler, R. Amino Diol HIV Protease Inhibitors. 1. Design, Synthesis, and Preliminary SAR. *J. Med. Chem.* **1994**, *37*, 1758−1768.
(47) Chen, P.; Cheng, P. T. W.; Alam, M.; Beyer, B. D.; Bisacchi, G. S.; Dejneka, T.; Evans, A. J.; Greytok, J. A.; Hermsmeier, M. A.; Humphreys, W. G.; Jacobs, G. A.; Kocy, O.; Lin, P. F.; Lis, K. A.; Marella, M. A.; Ryono, D. E.; Sheaffer, A. K.; Spergel, S. H.; Sun, C.; Tino, J. A.; Vite, G.; Colonno, R. J.; Zahler, R.; Barrish, J. C. Aminodiol HIV Protease Inhibitors. Synthesis And Structure−Activity Relationships Of P1/P1′ Compounds: Correlation between Lipophilicity and Cytotoxicity. *J. Med. Chem.* **1996**, *39*, 1991−2007.
(48) Ghosh, A. K.; Thompson, W. J.; McKee, S. P.; Duong, T. T.; Lyle, T. A.; Chen, J. C.; Darke, P. L.; Zugay, J. A.; Emini, E. A.; Schleif, W. A.; Huff, J. R.; Anderson, P. S. 3-Tetrahydrofuran and pyran urethanes as high-affinity P2-ligands for HIV-1 protease inhibitors. *J. Med. Chem.* **1993**, *36*, 292−294.
(49) Ghosh, A. K.; Kincaid, J. F.; Walters, D. E.; Chen, Y.; Chaudhuri, N. C.; Thompson, W. J.; Culberson, C.; Fitzgerald, P. M. D.; Lee, H. Y.; McKee, S. P.; Munson, P. M.; Duong, T. T.; Darke, P. L.; Zugay, J. A.; Schleif, W. A.; Axel, M. G.; Lin, J.; Huff, J. R. Nonpeptidal P2 Ligands for HIV Protease Inhibitors: Structure-Based Design, Synthesis, and Biological Evaluation. *J. Med. Chem.* **1996**, *39*, 3278−3290.
(50) Hagen, S.; Prasad, J. V. N. V.; Tait, B. D. Nonpeptide inhibitors of HIV protease. *Adv. Med. Chem.* **2000**, *5*, 159−195.
(51) Turner, S. R.; Strohbach, J. W.; Tommasi, R. A.; Aristoff, P. A.; Johnson, P. D.; Skulnick, H. I.; Dolak, L. A.; Seest, E. P.; Tomich, P. K.; Bohanon, M. J.; Horng, M. M.; Lynn, J. C.; Chong, K. T.; Hinshaw, R. R.; Watenpaugh, K. D.; Janakiraman, M. N.; Thaisrivongs, S. Tipranavir (PNU-140690): A Potent, Orally Bioavailable Nonpeptidic HIV Protease Inhibitor of the 5,6-Dihydro-4-hydroxy-2-pyrone Sulfonamide Class. *J. Med. Chem.* **1998**, *41*, 3467−3476 and references therein..
(52) Hagen, S. E.; Domagala, J.; Gajda, C.; Lovdahl, M.; Tait, B. D.; Wise, E.; Holler, T.; Hupe, D.; Nouhan, C.; Urumov, A.; Zeikus, G.; Zeikus, E.; Lunney, E. A.; Pavlovsky, A.; Gracheck, S. J.; Saunders, J.; VanderRoest, S.; Brodfuehrer, J. 4-Hydroxy-5,6-dihydropyrones as Inhibitors of HIV Protease: The Effect of Heterocyclic Substituents at C-6 on Antiviral Potency and Pharmacokinetic Parameters. *J. Med. Chem.* **2001**, *44*, 2319−2332.
(53) Wilkerson, W. W.; Dax, S.; Cheatham, W. W. Nonsymmetrically Substituted Cyclic Urea HIV Protease Inhibitors. *J. Med. Chem.* **1997**, *40*, 4079−4088.
(54) Dorsey, B. D.; McDonough, C.; McDaniel, S. L.; Levin, R. B.; Newton, C. L.; Hoffman, J. M.; Darke, P. L.; Zugay-Murphy, J. A.; Emini, E. A.; Schleif, W. A.; Olsen, D. B.; Stahlhut, M. W.; Rutkowski, C. A.; Kuo, L. C.; Lin, J. H.; Chen, I.-W.; Michleson, S. R.; Holloway, M. K.; Huff, J. R.; Vacca, J. P. Identification of MK-944a: A Second Clinical Candidate from the Hydroxylaminepentanamide Isostere Series of HIV Protease Inhibitors. *J. Med. Chem.* **2000**, *43*, 3386−3399.
(55) Lucca, G. V. D.; Liang, J.; Aldrich, P. E.; Calabrese, J.; Cordova, B.; Klabe, R. M.; Rayner, M. M.; Chang, C. H. Design, Synthesis, and Evaluation of Tetrahydropyrimidinones as an Example of a General Approach to Nonpeptide HIV Protease Inhibitors. *J. Med. Chem.* **1997**, *40*, 1707−1719.
(56) Solov'ev, V. P.; Varnek, A. Anti-HIV Activity of HEPT, TIBO, and Cyclic Urea Derivatives: Structure−Property Studies, Focused Combinatorial Library Generation, and Hits Selection Using Substructural Molecular Fragments Method. *J. Chem. Inf. Comput. Sci.* **2003**, *43*, 1703−1719.
(57) Debnath, A. K. Comparative Molecular Field Analysis (CoMFA) of a Series of Symmetrical Bis-Benzamide Cyclic Urea Derivatives as HIV-1 Protease Inhibitors. *J. Chem. Inf. Comput. Sci.* **1998**, *38*, 761−767.
(58) Han, Q.; Chang, C. H.; Li, R.; Ru, Y.; Jadhav, P. K.; Lam, P. Y. S. Cyclic HIV Protease Inhibitors: Design and Synthesis of Orally Bioavailable, Pyrazole P2/P2′ Cyclic Ureas with Improved Potency. *J. Med. Chem.* **1998**, *41*, 2019−2028.
(59) Jones, G.; Willett, P.; Glen, R. C.; Leach, A. R.; Taylor, R. Development and validation of a genetic algorithm for flexible docking. *J. Mol. Biol.* **1997**, *267*, 727−748.
(60) Case, D. A.; Darden, T. A.; Cheatham, T. E., III; Simmerling, C. L.; Wang, J.; Duke, R. E.; Luo, R.; Merz, K. M.; Wang, B.; Pearlman, D. A.; Crowley, M.; Brozell, S.; Tsui, V.; Gohlke, H.; Mongan, J.; Hornak, V.; Cui, G.; Beroza, P.; Schafmeister, C.; Caldwell, J. W.; Ross, W. S.; Kollman, P. A. *AMBER 8*; University of California, San Francisco: San Francisco, CA, 2004.
(61) Jakalian, A.; Bush, B. L.; Jack, D. B.; Bayly, C. I. Fast, efficient generation of high-quality atomic charges. AM1-BCC Model. *J. Comput. Chem.* **2000**, *21*, 132−146.
(62) Wang, J.; Wolf, R. M.; Caldwell, J. W.; Kollman, P. A.; Case, D. A. Development and testing of a general Amber force field. *J. Comput. Chem.* **2004**, *25*, 1157−1174.
(63) Hou, T.; Yu, R. Molecular Dynamics and Free Energy Studies on the Wild-type and Double Mutant HIV-1 Protease Complexed with Amprenavir and Two Amprenavir-Related Inhibitors:? Mechanism for Binding and Drug Resistance. *J. Med. Chem.* **2007**, *50*, 1177−1188.
(64) Fong, P.; McNamara, J. P.; Hillier, I. H.; Bryce, R. A. Assessment of QM/MM Scoring Functions for Molecular Docking to HIV-1 Protease. *J. Chem. Inf. Model.* **2009**, *49*, 913−924.
(65) Li, D.; Ji, B.; Hwang, K. C.; Huang, Y. Strength of Hydrogen Bond Network Takes Crucial Roles in the Dissociation Process of Inhibitors from the HIV-1 Protease Binding Pocket. *PLoS One* **2011**, *6*, e19268.
(66) Huang, D.; Caflisch, A. How Does Darunavir Prevent HIV-1 Protease Dimerization? *J. Chem. Theory Comput.* **2012**, *8*, 1786−1794.
(67) Darden, T.; York, D.; Pederson, L. Particle mesh Ewald: An N·log(N) method for Ewald sums in large systems. *J. Chem. Phys.* **1993**, *98*, 10089−10092.
(68) *SYBYL 6.9.2*; Tripos Inc.: St. Louis, MO, 2004.
(69) Shen, C. H.; Wang, Y. F.; Kovalevsky, A. Y.; Harrison, R. W.; Weber, I. T. Amprenavir complexes with HIV-1 protease and its drug-resistant mutants altering hydrophobic clusters. *FEBS J.* **2010**, *277*, 3699−3714.
(70) Luo, R.; David, L.; Gilson, M. K. Accelerated Poisson-Boltzmann calculations for static and dynamic systems. *J. Comput. Chem.* **2002**, *23*, 1244−1253.
(71) *Maestro*, version 8.5; Schrödinger, LLC: New York, NY, 2008.
(72) DeGorter, M. K.; Xia, C. Q.; Yang, J. J.; Kim, R. B. Drug Transporters in Drug Efficacy and Toxicity. *Annu. Rev. Pharmacol. Toxicol.* **2012**, *52*, 249−273.
(73) http://www.fda.gov/forconsumers/byaudience/forpatientadvocates/hivandaidsactivities/ucm118915.htm (accessed August 16, 2012).